physchem

MDPI

Article

The Surprising Role of Endogenous Calcium Carbonate in Crab Shell-Mediated Biosorption of Pb (II)

Carolina Londoño-Zuluaga [1,2], Hasan Jameel [1], Ronalds W. Gonzalez [1], Guihua Yang [2,*] and Lucian Lucia [1,2,3,4,*]

[1] Department of Forest Biomaterials, North Carolina State University, Raleigh, NC 27695, USA; carolina.londonozu@gmail.com (C.L.-Z.); jameel@ncsu.edu (H.J.); rwgonzal@ncsu.edu (R.W.G.)
[2] Key Laboratory of Bio-Based Materials & Green Papermaking, Qilu University of Technology, Jinan 250535, China
[3] Department of Chemistry, North Carolina State University, Raleigh, NC 27695, USA
[4] Joint Department of Biomedical Engineering, North Carolina State University, Raleigh, NC 27695, USA
* Correspondence: ygh2626@126.com (G.Y.); lalucia@ncsu.edu (L.L.)

Abstract: Crustacean shells, waste from the seafood industry, have been identified as a potential sustainable material for the adsorption of lead, a potent heavy metal found in the discharge of industrial processes. The dynamics and kinetics of its performance were evaluated in batch experiments under pH, temperature, time, and initial concentration. A unique and non-intuitive key finding was that among the native components of the crab shell matrix, i.e., chitin, protein, and calcium carbonate, calcium carbonate was instrumental in sequestration. The role of protein was minimal, whereas the efficiency of chitin in lead complexation was linked to the lead atomic radius, which, of the crab shell components, we determined was very prone to interacting with chitin.

Keywords: biosorption; dynamics; kinetics; Langmuir and Freundlich isotherms; crab shell; chitin; calcium carbonate; Pb (II)

check for updates

Citation: Londoño-Zuluaga, C.; Jameel, H.; Gonzalez, R.W.; Yang, G.; Lucia, L. The Surprising Role of Endogenous Calcium Carbonate in Crab Shell-Mediated Biosorption of Pb (II). *Physchem* **2024**, *4*, 167–180. https://doi.org/10.3390/physchem4020013

Academic Editors: Francesco Mallamace and James A. Platts

Received: 26 July 2022
Revised: 23 November 2023
Accepted: 5 June 2024
Published: 20 June 2024

Copyright: © 2024 by the authors. Licensee MDPI, Basel, Switzerland. This article is an open access article distributed under the terms and conditions of the Creative Commons Attribution (CC BY) license (https://creativecommons.org/licenses/by/4.0/).

1. Introduction

Increasing human activity and industrialization are currently the main point sources of pollutants in the environment. Large volumes of effluents containing heavy metals, radioactive waste, and organic pollutants are discharged into natural watersheds that eventually contaminate soils, wildlife, fish, and humans [1]. Heavy metals such as lead are among the most persistent and incalcitrant contaminants compared to organic compounds and petroleum derivatives [2] facilitating transit through the food chain [3] and eventually resulting in heavy metal poisoning.

An earlier batch experiment study examined whether compost and biogas residues could bio-sorb and remove lead (Pb) from contaminated water [4]. Biosorption was found to decrease with increasing Pb concentration, but at equilibrium, relatively greater sorption and removal were observed from compost compared to biogas fit by the Freundlich equilibrium adsorption isotherm model. Compost was more porous, had greater surface area compared to biogas, and showed great sorption potential.

Heavy metal poisoning from lead is a consequence of exposure to contaminated water, food, or air [2]. Although several heavy metals are needed for human life (e.g., selenium), higher levels can lead to adverse effects. Today, thirty-five metals have been classified as threats to human health, of which twenty-three are heavy metals [5] whose intake through drinking water can lead to cancer, heart diseases, anemia, and kidney and liver damage [6,7]. Among heavy metals, lead, cadmium, and arsenic stand out for their high toxicity and are among the most common heavy metals that cause human poisoning. Lead is the most commonly found in water, especially due to the presence of this metal in plumbing material that corrodes under acidic conditions and in low mineral water, eventually finding its way

into streams. According to the Environmental Protection Agency (EPA), even at low levels, lead poisoning can result in behavior and learning problems, seizures, anemia and slow growth in children, premature births in pregnant women, liver damage, reduced pulmonary function, lung dysfunction, gastrointestinal disorders, and cardiovascular dysfunction in adults. Although the consequences of heavy metal consumption by humans are well known, removing them from water remains a challenge. Common water remediation technologies include chemical precipitation and electrochemical treatment; however, these methods are largely amenable to relatively high heavy metal concentrations.

Additional technologies include membrane filtration and activated carbons, zeolites, or synthetic polymers; however, these latter technologies are expensive because they are highly dependent on the availability of raw materials [8]. Adsorption with activated carbon is commonly used because it provides a large pore size distribution and large surface area; nonetheless, large energy consumption and low yields conspire to deliver an expensive product for treating large amounts of water [8]. Consequently, activated carbon, even though effective, is unfeasible for large-scale applications. It is also unaffordable for low-to-medium-income communities [9].

New materials for heavy metal removal have been studied to assess technical feasibility and economics. Biosorption, the use of biological materials for adsorption [10], has been an intense subject of study for a variety of reasons [11]. Biomaterials have been studied as potential low-cost adsorbents because they have high metal binding capacities, are ubiquitous, inexpensive, and incur low processing costs [12]. Examples of such biomaterials include algae [9], microorganisms [12], bacteria [11], and biomass from fruit peels, bagasse, black liquor, and crustacean shells [8].

Interestingly, crustacean shells contain sequestrants such as chitin but have been sparingly studied as heavy metal sequesters despite being a low-cost option and being available in large quantities as a waste by-product of the seafood industry [13]. It is estimated that 6–8 million tons of crab, shrimp, and lobster shells are produced every year [14]. Typically, crustacean shells are disposed of in landfills because there is little data suggesting that they have the potential for valorization; however, landfilling tipping costs in several countries are high [14]. Alternative value-added uses have been considered, including chemical treatment to produce fertilizers [15,16], animal feed [17], and heavy metal ion sequesters [18]. The current work focused on studying the dynamics and kinetics of the removal of lead using pulverized crab shells whose performance was evaluated at high and low concentrations with concomitant material characterization.

2. Materials and Methods

2.1. Materials

Crab shells were purchased from a seafood processing company whose identity is not disclosed to maintain confidentiality. Sodium hydroxide, hydrochloric acid, and lead (Pb) (II) nitrate were purchased from VWR and used as received unless otherwise specified.

2.2. Methods

Shell cleaning and particle size reduction. Crab shells were washed and cleaned using deionized water and oven-dried at 60 °C for 24 h. Particle size reduction was performed using a Wiley mill until 40-mesh particle sizes were obtained.

Compositional Analysis. Raw material (crab shell) characterization was performed to determine major chemical composition (i.e., protein, calcium carbonate, and chitin). Mass balance was performed through the extraction of each major component in the crab shell. Proteins were extracted by treating the crushed crab shells with a 1 M solution of sodium hydroxide at 65 °C for 2 h. Subsequently, the residual calcium carbonate and other minerals were removed by acid treatment using 1.5 M hydrochloric acid at room temperature for

5 h. Elemental analysis was used to measure the amount of N and Ca. The results were translated to protein content using the following equation:

$$\%P = (\%N - 6.9) \times 6.25 \quad (1)$$

where %P is the fraction of protein and %N is the fraction of nitrogen reported by elemental analysis, which was obtained using a Perkin Elmer 2400 CHNS Analyzer (Perkin Elmer, Waltham, MA, USA). The number 6.9 corresponds to the theoretical percentage of N on fully acetylated chitin while 6.5 corresponds to the theoretical percentage of N in proteins [19].

Fourier-transform infrared spectroscopy (FTIR). The analysis of functional groups present in the composite material was accomplished using UATR in a PerkinElmer Frontier IR single-beam spectrometer. The window used for the analysis was 4000–650 cm^{-1} at a resolution of 4 cm^{-1} and 32 scans.

X-ray Diffraction (XRD). A Rigaku Smart Lab X-ray diffractometer was used for XRD measurements of powdered samples. The experiments were carried out at 2θ = 5–40° [20].

Scanning electron microscopy (SEM). Morphological analyses of the samples were performed using a Field Emission Scanning Electron Microscope–FEI Verios 460L (Field Electron and Ion Company, Hillsboro, OR, USA). A voltage of 1.00 kV and 13 pA current were used. For higher magnification samples, a 500 V bias was used to reduce sample charging.

Energy-dispersive X-ray spectroscopy (EDX). Elemental Analysis was performed using an Oxford energy-dispersive X-ray in a variable pressure scanning electron microscope (VP-SEM) Hitachi S3200N (Hitachi, Tokyo, Japan).

Brunauer–Emmett–Teller (BET). The specific surface area (BET) of the sample was measured with a Micromeritics Gemini VII 2390p instrument (Norcross, GA, USA), using the adsorption of N_2 at 77 K according to the literature [21].

Batch Experiments. Crab shells were grounded and used as an adsorbent for the removal of Pb (II). Metal uptake (mg/g), q_e, was used to assess the performance of the ground crab shells. To evaluate the basis for its sorption performance, pH, adsorbent dose, contact time, and temperature were controlled. Pb (II) concentration was measured using an ICP-MS (Inductively Coupled Plasma Mass Spectrometry) Perkin Elmer Elan DRCII. The following equations were used to express the efficiency of the adsorption of Pb (II):

$$q_e = \frac{V \times (C_0 - C_e)}{W} \quad (2)$$

$$\%\text{Removal} = \frac{C_0 - C_e}{C_0} \times 100\% \quad (3)$$

where q_e is metal uptake (mg/g), V is the volume of the solution (mL), W is the weight of the crab shell (g), C_0 is the concentration of Pb (II) before adsorption (mg/mL), and C_e is the concentration of Pb (II) after adsorption (mg/mL).

Effect of pH. Pb (II) uptake was determined at different pHs, which were controlled using diluted solutions of hydrochloric acid (HCl) and sodium hydroxide (NaOH).

Effect of adsorbent dose. Masses of crab shells (0.1–1.0 g) were placed in contact with the Pb (II) solution for 1 h after which q_e was determined.

Effect of contact time. Standard masses of adsorbent were placed in contact with the Pb (II) solution at 10–240 min intervals.

Effect of temperature. To analyze the thermodynamic behavior of adsorption, the effect of the temperature was measured from 20 to 40 °C.

Adsorption Isotherms. Adsorption was evaluated using a variable concentration of Pb (II), from 10 mg/L to 1000 mg/L, and data obtained were fitted according to linear Langmuir and Freundlich isotherm models. The monomolecular adsorption of a single

metal from a liquid to a solid was modeled using Langmuir and Freundlich adsorption isotherm models [22]:

$$q_e = \frac{q_{max} b C_e}{1 + b C_e} \quad (4)$$

where q_{max} is the maximum metal uptake (mg/g), b is the Langmuir equilibrium constant related to the affinity of binding sites, which measures the energy of adsorption (L/mg), and C_e is the final concentration of the metal in the solution. The linearized form of Equation (4) is:

$$\frac{C_e}{q_e} = \frac{1}{q_{max} b} + \frac{C_e}{q_{max}} \quad (5)$$

In our work, the Freundlich isotherm represents an empirical equation assuming adsorption on a heterogeneous crab shell–water interface possessing an adsorption capacity as a function of the concentration of adsorbed lead cations at equilibrium. This isotherm is best for treating metal ion adsorption at high concentrations, as represented by Equation (6):

$$q_e = K_f C_e^{1/n} \quad (6)$$

where q_e is the metal uptake (mg/g), K_f is the adsorption capacity at unit concentration (L/mg), 1/n is the strength of adsorption, and C_e is the final concentration of the metal in the solution and may be linearized according to Equation (7):

$$\ln q_e = \frac{1}{n} \ln C_e + \ln K_f \quad (7)$$

3. Results and Discussion

Characterization. An important objective of our characterization studies was determining the main components of the raw material and their role in Pb (II) biosorption. In theory, crab shells and crustacean shells are comprised almost exclusively of calcium carbonate, protein, and chitin [23]. The level of each component varies depending on the species. After acid extraction with hydrochloric acid (1.5 M), calcium carbonate composed 68% of the total mass. The protein content was determined using the bicinchoninic acid (BCA) assay for protein analysis and elemental analysis after alkali treatment (1 M). The protein content was determined to be 8.4%. Chitin content was determined to be 15.1%, whereas the water content was 6.4% on a dry basis. The crab shell composition was found to be comparable to previous reports [24].

Fourier-transform infrared spectroscopy (FTIR). FTIR spectra (Figure 1) were used to identify key functional groups in chitin and crab shells. For chitin, distinct peaks at 3443, 3259, 1656, 1625, and 1553 cm^{-1} were observed that are attributed to the stretching of OH groups, NH groups, and amide I and amide II, respectively [25,26]. In crab shells, peaks at 3262, 1635, 1420, 1052, and 872 were observed, attributed to NH stretching, -N-H-CO stretching, NO_2 groups in protein, and calcium carbonate, respectively [27,28].

X-ray Diffraction (XRD). Among crab shell components, calcium carbonate and chitin crystal structures can diffract X-rays. Peaks with higher intensity are associated with one of these latter structures. In samples of pure crab shell, the peak at 2θ~30° is associated with the presence of calcium carbonate in its polymorphic structures; calcite [29] at room temperature is the most thermodynamically stable form of $CaCO_3$ [30].

Alternatively, for pure chitin samples, the main peaks found at 2θ~9.15–9.25° and 19.05–19.15° are associated with amorphous and crystalline diffractions of chitin, respectively. These peaks serve to assess the crystallinity index of the chitin structure based on Equation (2), in which chitin was found to be 0.54. Together with the results from FTIR and what is already reported, the structure of the crab shell corresponds to an α-chitin polymorph [31].

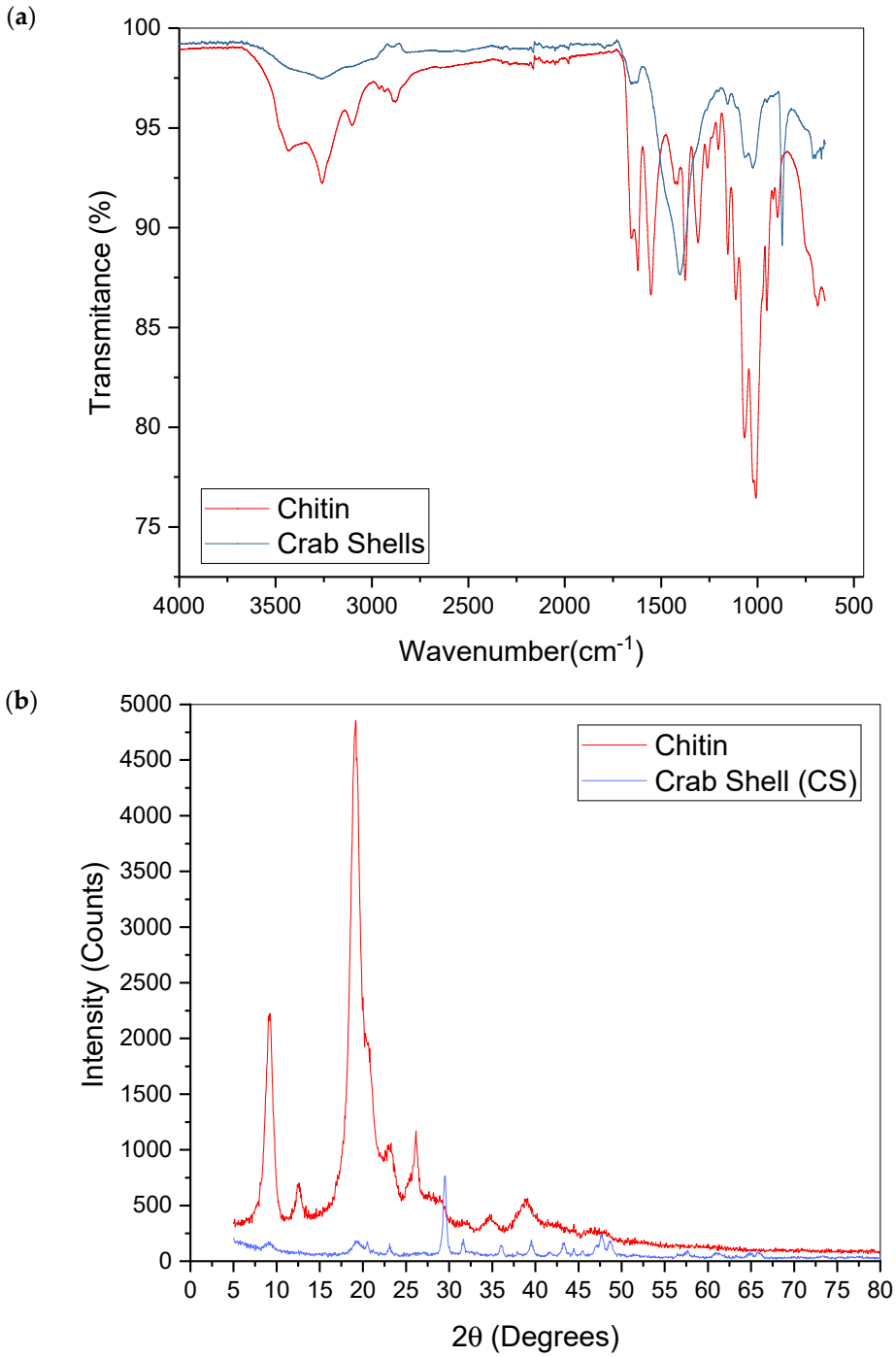


Figure 1. (**a**) LEFT: FTIR spectra of chitin and crab shells. (**b**) RIGHT: X-ray diffraction for pure crab shell and pure chitin. The XRD patterns of all types of chitosan display two crystalline peaks at 2θ = 10° and 20° [32].

3.1. Scanning Electron Microscopy (SEM)

Scanning electron microscopy was used to determine material morphology. In Figure 2a, crab shells display three external layers. The first is the epicuticle, a mostly waterproof barrier, followed by the exocuticle, which supports mechanical loads, and finally, the endocuticle, which is ~90% of the shell [31]. In a more detailed image, Figure 2b, chitin fibers whose general orientation is apparent can be observed. A porous structure, responsible for nutrient transport within the structure, can be observed. The pores extant throughout the endocuticle are approximately 30–50 nm in size, spaced ~5 nm apart, and account for ~70% porosity.

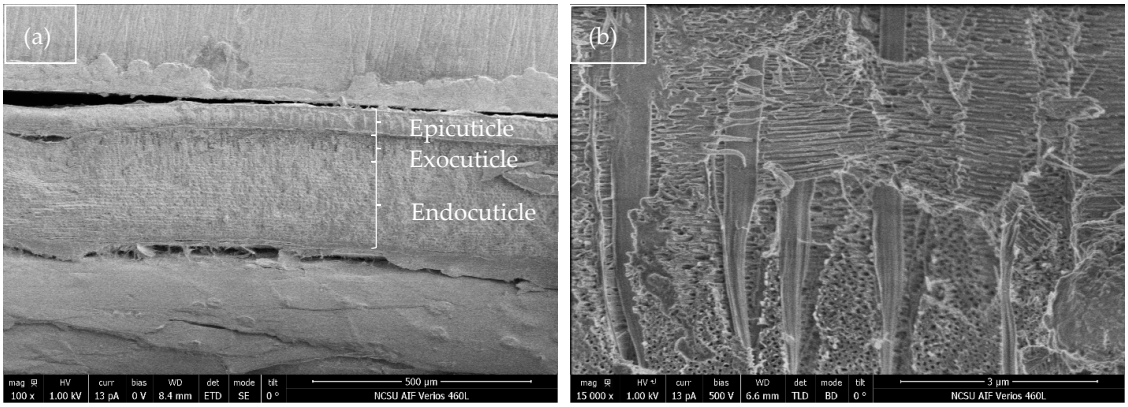


Figure 2. SEM images of (**a**) Crab Shell at 100×, 500 µm. (**b**) Crab Shell at 15,000×, 3 µm.

3.2. Batch Experiments

3.2.1. High Lead Concentration (100 mg/L)

Adsorbent concentration, contact time, pH, and temperature effects were evaluated. As observed in Figure 3, under constant pH, initial concentration, contact time, and temperature, the increased addition of adsorbent decreased the adsorption capacity of lead due to steady-state saturation kinetics. With respect to contact time, longer times allow for increasing adsorption, in which the removal efficiency varies from 98.66% after one hour to 99.32% after four hours; the adsorption capacity changes from 25.5 to 26.5 mg/g. Our result is very much in line with experimental data obtained using rapeseed sorbents for Pb (II), in which a Pb (II) removal efficiency of 94.47% was obtained [33].

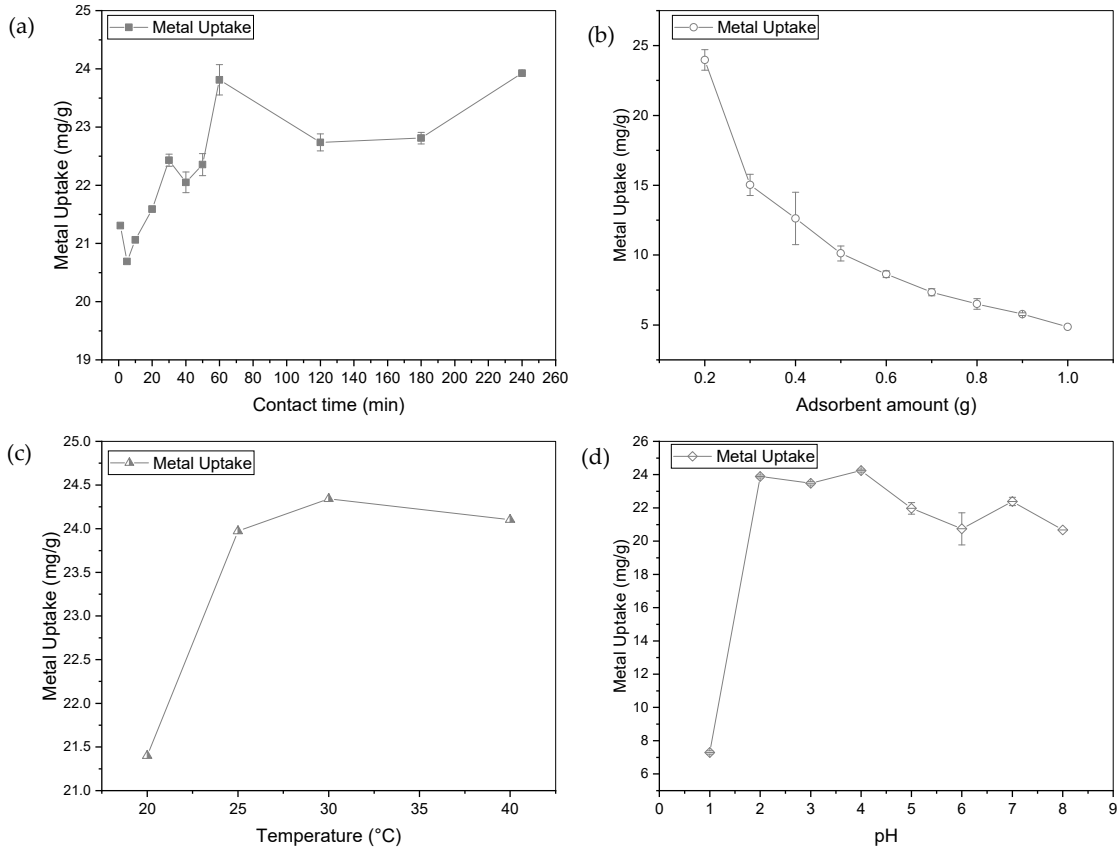


Figure 3. Effects of different adsorption parameters on the biosorption capacity of lead by crab shells, with 100 mg/L of lead as the starting concentration. (**a**) Contact time, (**b**) Adsorbent amount, (**c**) Temperature, (**d**) pH.

With respect to pH, higher adsorption is achieved for pH between 3 and 4. These phenomena are likely due to the pH speciation of lead within this pH range, which allows precipitation on the surface of the crab shell followed by sequestration. This is not an altogether surprising finding given what has already been reported [33]. Acidic pH also significantly helps in the ionization of calcium carbonate, favoring a variety of complexations between lead and calcium carbonate. A temperature of ~30 °C was optimal for biosorption in our limited temperature range, although it was only 10–15% greater than what was observed at room temperature; therefore, the influence of temperature is not as important as the other parameters studied, which is not completely surprising.

3.2.2. Low Lead Concentration (10 mg/L)

Common concentrations of lead in raw drinking water are in the range of 10 mg/L. However, most adsorbents fail to remove heavy metals at this concentration. Consequently, we decided to evaluate the performance of heavy metal ions at concentrations starting from 10 mg/L, where a plateau of ~0.2 mg/L was achieved. In Figure 4, similar conditions used for high lead concentrations (Figure 3) were evaluated at low lead concentrations. As a result, maximum metal uptake corresponded to 42 mg/g at 10 mg of material; pH 5 was ideal at ~60 min of residence time, which appears to correspond to an optimal pH for lead precipitation at the calcium carbonate sites in the crab shells. The conditions were evaluated at pH values obtained from optimization studies conducted under high lead concentrations. Because pH changes the speciation of lead in water to favor its precipitation at higher pHs, it was reasonable to discover similar behavior at low lead concentrations. Remarkably, at a 10 mg/L (low) lead concentration, we observed a much faster kinetic response relative to the 100 mg/L (high) concentration of lead which likely has to do with the more abundant site (calcium carbonate) adsorption access (saturation kinetics), a finding which is not surprising.

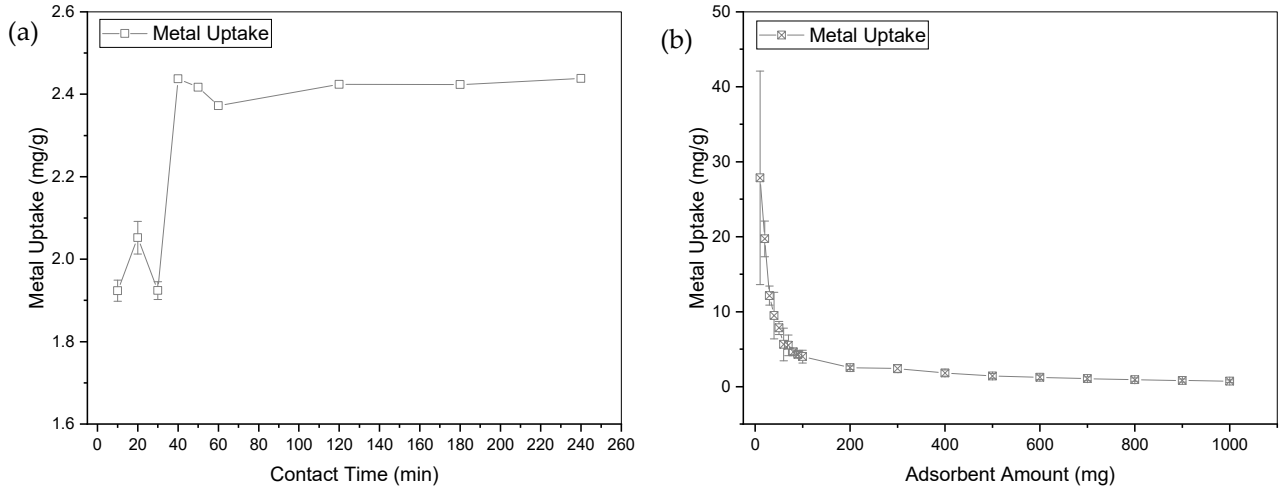


Figure 4. Effects of different adsorption parameters on the adsorption capacity of lead by crab shells when using 10 mg/L of lead as the starting concentration. (**a**) Contact time, (**b**) Adsorbent amount.

3.3. Energy-Dispersive X-ray Spectroscopy (EDS)

EDS Analysis was used to estimate the final concentrations of different elements on the crab shell surface. As shown in Figure 5, the presence of lead can be observed on the surface. Additionally, it is important to consider the peaks associated with calcium since this element plays a central role in the adsorption process.

The calcium on the surface is mainly due to the calcium carbonate and is the basis for the bio-sorption phenomenon of crab shells. As shown by the acid pH experiments, the main mechanism for the removal of heavy metals is cation exchange between the calcium cation of the carbonate salt and the metal ions. In the end, the expected outcome is the precipitation of (Pb, Ca)-CO_3 compounds on the surface, a sequestration phenomenon that

ensures the removal of Pb (II). This result was shown to be the case for not only lead but also for other heavy metal ions, which were removed by calcium-enriched sorbents [34].

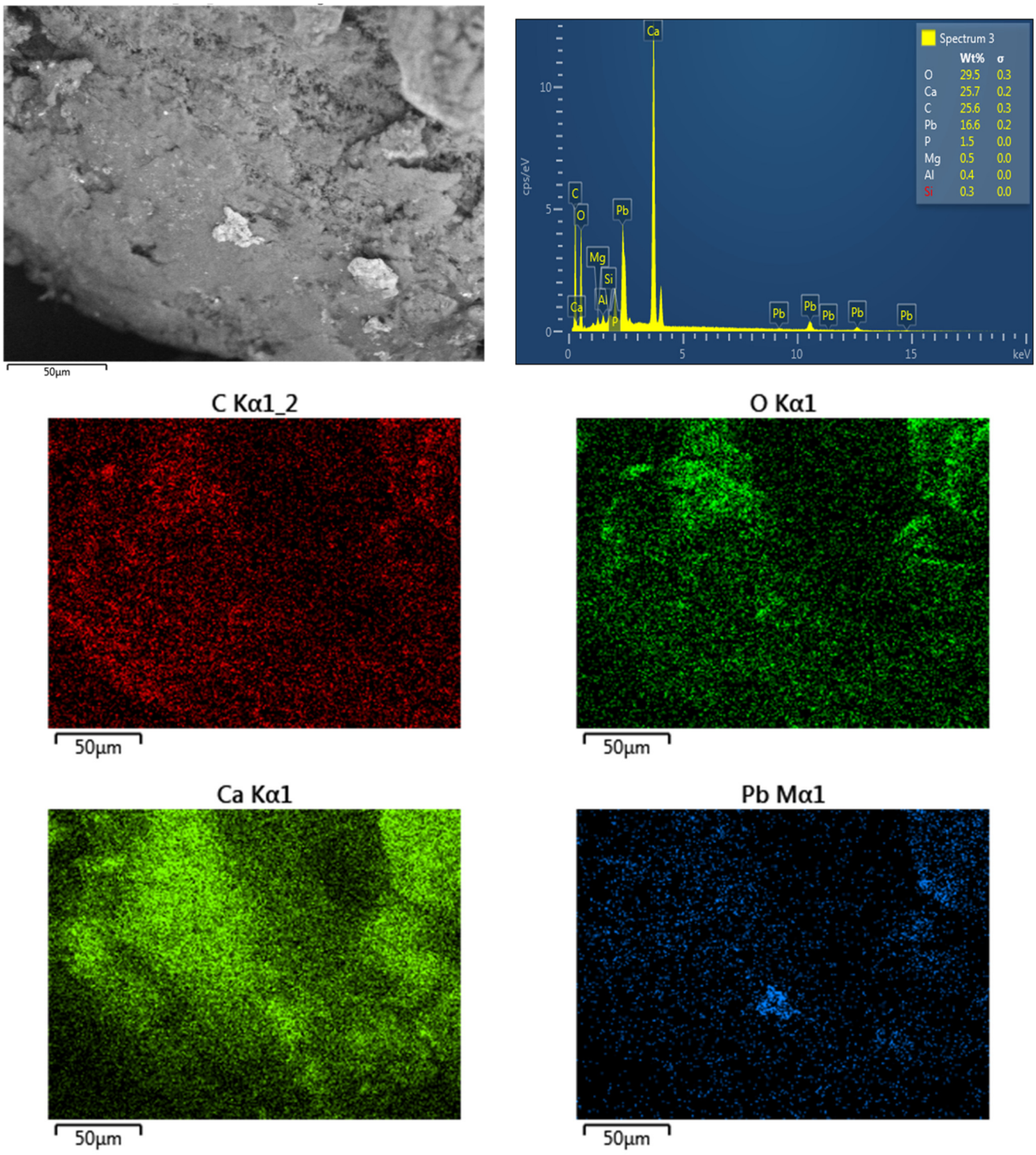


Figure 5. SEM-EDS of crab shell bio-sorbents after lead adsorption.

3.4. Adsorption Isotherms

The adsorption isotherm deconvolves adsorption mechanisms on how adsorbates such as lead distribute between the liquid and the crab shell. Langmuir isotherm assumes two adsorption process foundational principles: (1) adsorption occurs at specified homogeneous adsorption sites, and (2) monolayer adsorption with concomitant maximum adsorption occurs when adsorbates (lead cations) form a saturated layer. It is understood all adsorption

sites are energetically the same and intermolecular forces diminish with an inverse square function of the distance to the adsorption site.

In our study, the Langmuir and Freundlich models were used to assess the adsorption equilibrium between the lead cation and the crab shell biosorbent. The isotherm constants for the two models were obtained using the linear regression method and are listed in Table 1. Once optimal results for adsorption of lead were obtained, adsorption isotherms were evaluated according to pH, residence times, and sorbent levels. The adsorption isotherm is shown in Figure 6, where the experimental data were fitted according to linearized Langmuir and Freundlich isotherms as shown in Equations (5) and (7), respectively. The maximum adsorption capacity, q_{max}, using the Langmuir model was 384.6 mg/g (Table 1). In this case, the system has an $R^2 > 0.99$ goodness of fit to the Langmuir isotherm, which assumes monolayer adsorption at least in one part of the process, followed by multilayer adsorption, as later confirmed by BET studies conducted to confirm that the absorption models are valid.

Table 1. Results of Langmuir and Freundlich isotherm linear model parameters †.

Regression Parameter	Langmuir Isotherm	Freundlich Isotherm
$1/q_{max}$ b	0.32	N/A
q_{max} (mg/g)	384.60	N/A
b	0.01	N/A
ln K_f	N/A	0.89
K_f	N/A	7.76
n	N/A	1.56

† Each of the linearized isotherms had $R^2 = 0.95$.

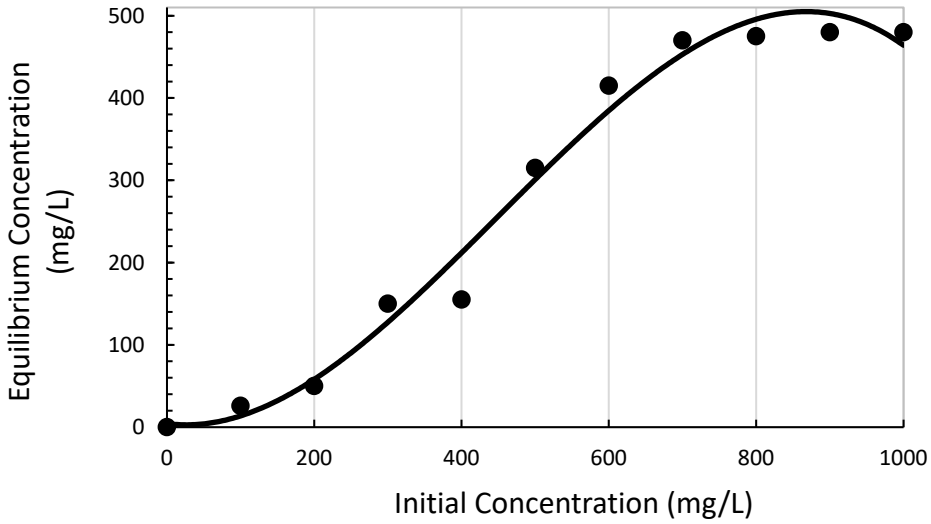


Figure 6. A graph of a typical adsorption isotherm in which the errors of the equilibrium concentrations are <5%.

Metal adsorption occurs via the formation of a lead cation monolayer on a crab shell surface with a finite number of identical sites that are homogeneously distributed. Freundlich provides two parameters, K_f and n, in which K_f is a function of the adsorption capacity and intensity of lead cations on the crab shell and represents the number of metal ions adsorbed at equilibrium concentration, and n represents the strength of Pb (II) adsorption, in which a value from 1 to 10 indicates relatively strong adsorption (in our case, n = 1.56).

3.5. Kinetic Studies

Kinetics provide valuable data on the mechanism of biosorption to tune the efficiency of adsorption. A variety of kinetic models are available, including pseudo-first-order,

pseudo-second-order, and intraparticle diffusion, to examine the controlling mechanisms of biosorption (e.g., chemical reactivity, diffusion, and mass transfer). A pseudo-first-order equation is expressed in Equation (8):

$$\frac{dq_{tdt}}{dt} = k_1(q_e - q_t) \quad (8)$$

where k_1 is the equilibrium rate constant of a pseudo-first-order kinetic model (min^{-1}). Following integration and recognition of the validity of the conditions, $q_t = 0$ at $t = 0$ and $q_t = q_t$ at $t = t$, a linearized differential equation may be obtained as follows:

$$\log(q_e - q_t) = \log q_e - \frac{k_1}{2.303}t \quad (9)$$

Straight-line plots of $\log(q_e - q_t)$ versus t for the biosorption of Pb (II) onto crab shell at Pb(II) concentrations of 10, 50, and 100 mg/L were tested to obtain rate parameters whose results are shown in Table 2.

Table 2. Kinetic parameters of pseudo-first-order and pseudo-second-order models of Pb (II) removal by crab shells at 25 °C.

Pseudo-First-Order Fit		**Pseudo-Second-Order Fit**		
Slope	R^2	q_e	k_2	R^2
−0.0008	0.9429	77.69	0.001	0.9936

Data were later subjected to a pseudo-second-order kinetic rate equation expressed as follows:

$$\frac{t}{q_t} = \frac{1}{k_2 {q_e}^2} + \frac{t}{q_e} \quad (10)$$

where k_2 is the equilibrium rate constant of a pseudo-second-order kinetic model (g/mg × min). The applicability of the model was tested by drawing linear plots of $\frac{t}{q_t}$ versus t at different Pb (II) concentrations (10, 50, and 100 mg/L) on the crab shell. k_2, q_e, and R^2 (correlation coefficient) were calculated from all plots and are given in Table 2.

Data in Table 2 clearly demonstrate the inapplicability of the pseudo-first-order kinetic model for the adsorption of Pb (II) on crab shells due to the negative slope and lower R^2. However, the linear fit of t/qt versus contact time (t), as indicated by the tight correlation coefficient ($R^2 > 0.99$) of the pseudo-second-order kinetic model, shows the applicability of this model, which demonstrates that initial Pb (II) concentration has an important role in the adsorption capacity of the crab shell.

3.6. BET Surface Area

BET analysis was performed with the objective of determining the surface area values of the materials along with the types of adsorption. As a result, it is possible to ascertain the porosity of the solid. In Table 3, results associated with the total surface area can be observed for crab shells and crab shells after alkali treatment (no protein) and acid treatment. In relation to the results obtained using ICP-MS, higher adsorption by crab shells is obtained once proteins are removed. This phenomenon takes place because, after protein removal, the calcium carbonate is more exposed, thus allowing significantly higher interaction with Pb (II).

Alternatively, analysis of the relative pressure vs. adsorption gives an idea of the type of adsorption. As shown in Figure 7, the behavior of crab shell adsorption is more like a type II adsorption isotherm. In this case, at low pressure, there is the formation of a monolayer, while at high pressure, multilayer adsorption takes place. As a result, it is possible to infer a macroporous structure within the crab shell [35].

Table 3. BET surface area results with $R^2 = 0.95$.

Material Characteristics	Surface Area (m^2/g)
Crab Shell 40 mesh	28.7
Crab Shell No Protein (No Protein)	49.1
Crab Shell No Mineral (No $CaCO_3$)	2.2

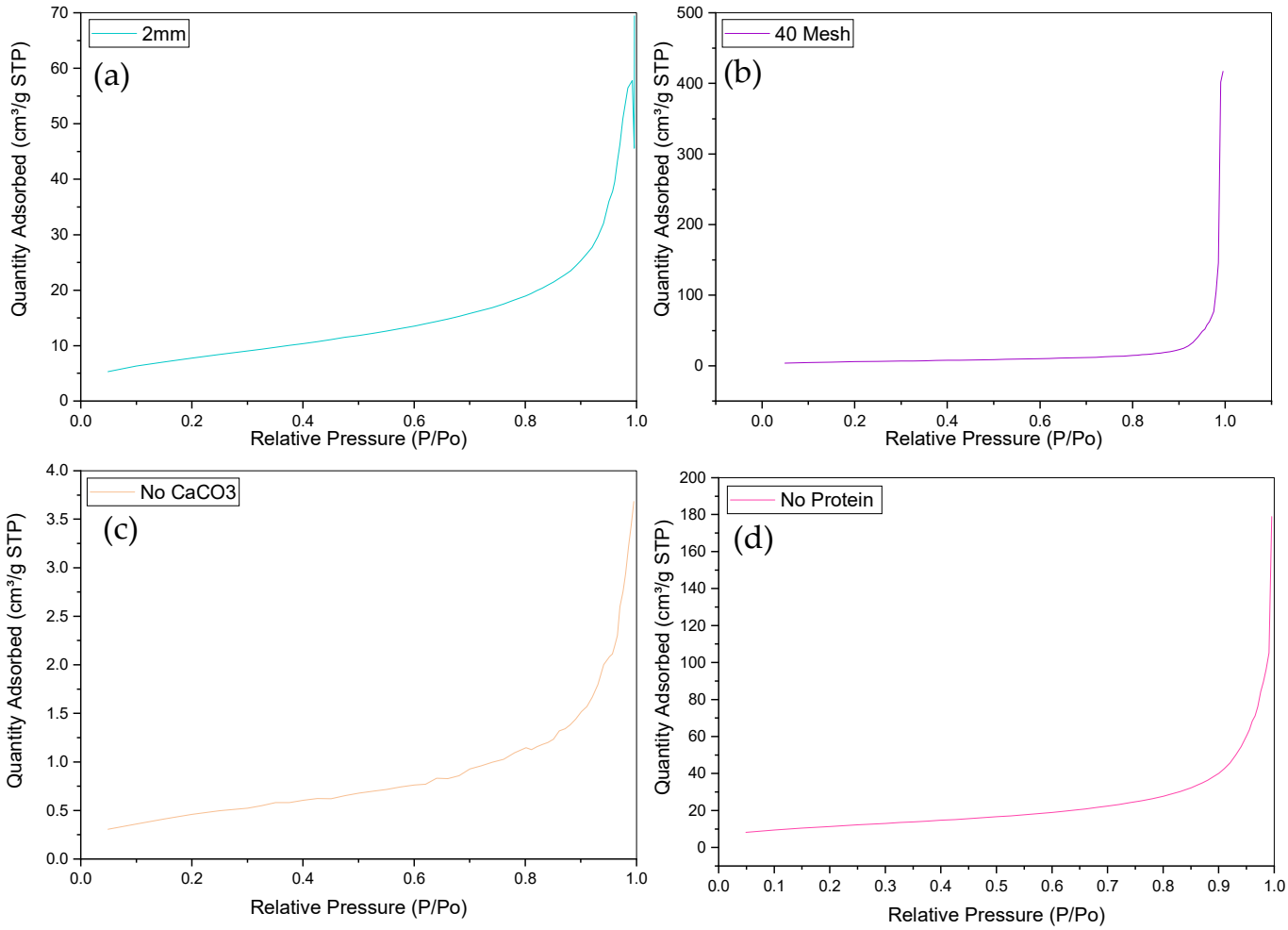


Figure 7. Relative pressure vs. quantity adsorbed for (**a**) Crab shell, 2 mm, (**b**) Crab shell, 40 mesh, (**c**) Crab shell, no $CaCO_3$, (**d**) Crab shell, No protein.

3.7. Additional Extraction Studies

In the search for possible explanations for the behavior shown, three additional tests were performed (Figure 8). Calcium carbonate and proteins were removed from the matrix of the crab shells, which were then re-evaluated to scrutinize performance. It was found that higher adsorption was achieved when proteins were removed from the crab shells. Therefore, it can be safely stated that calcium carbonate plays a key role in the adsorption of Pb (II) through the formation of different compounds between Pb (II) and calcium carbonate as supported by previous studies [18]. The mechanism behind the removal is based on ion exchange followed by precipitation of Pb (II)–carbonate compounds in addition to complexation with chitin.

Finally, chitin plays a key role in the adsorption process via the complexation of Pb (II); in fact, its efficiency has been linked to the radius and the size of the molecule [36,37]. Bigger contaminants such as lead, for example, are more likely to interact with chitin. This is, in part, supported by our previous studies [38,39].

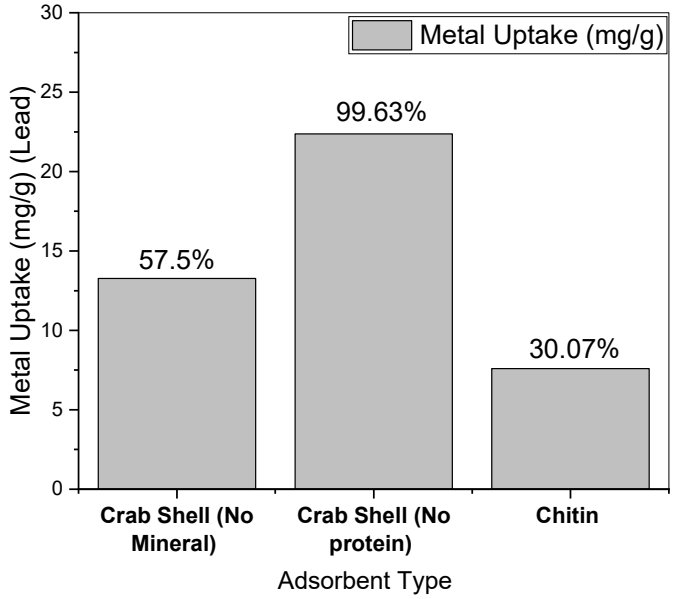


Figure 8. Pb (II) adsorption by partially modified crab shells. Error is within ±5%.

4. Conclusions

The crab shell was shown to represent a unique sorption platform for Pb (II) removal by virtue of its compositional characteristics. A key finding was that among its native components, calcium carbonate was instrumental in sequestration, whereas the role of protein was marginal at best. Interestingly, a non-intuitive finding was that despite the rich amine functionalization of chitin, complexation was associated with ionic radius, which was more likely, therefore, to interact with chitin. Nevertheless, the most remarkable finding in this study is that calcium carbonate appears to be extremely versatile in providing biosorption. It was found that acidic pH helps in the ionization of calcium carbonate (calcite), favoring complexation between Pb (II) and calcium carbonate ions. In addition, the removal of the protein layer significantly enhanced the exposure of the calcite structure, allowing for increased sequestration.

Author Contributions: Conceptualization, L.L.; methodology, C.L.-Z.; software, G.Y.; validation, H.J. and R.W.G.; formal analysis, L.L.; investigation, H.J., R.W.G., G.Y. and L.L.; resources, L.L. and G.Y.; data curation, C.L.-Z.; writing—original draft preparation, C.L.-Z.; writing—review and editing, L.L. and G.Y.; visualization, C.L.-Z.; supervision, H.J., R.W.G. and L.L.; project administration, L.L.; funding acquisition, L.L., R.W.G. and H.J. All authors have read and agreed to the published version of the manuscript.

Funding: We acknowledge NC Biotechnology Center (Grant No. 571068), whose generous support made portions of this work possible. This work was performed in part at the Analytical Instrumentation Facility (AIF) at North Carolina State University, which is supported by the State of North Carolina and the National Science Foundation (award number ECCS-1542015). The AIF is a member of the North Carolina Research Triangle Nanotechnology Network (RTNN), a site in the National Nanotechnology Coordinated Infrastructure (NNCI).

Data Availability Statement: Data are contained within the article.

Acknowledgments: This work was also performed in part at the Environmental and Agricultural Testing Service Laboratory (EATS), Department of Crop and Soil Sciences, at North Carolina State University and Mass Spectrometry CORE Laboratory, Chemical Research Instrumentation Teaching & Core Labs (CRiTCL), at University of North Carolina-Chapel Hill.

Conflicts of Interest: The authors declare no conflict of interest.

References

1. Fomina, M.; Gadd, G.M. Biosorption: Current Perspectives on Concept, Definition and Application. *Bioresour. Technol.* **2014**, *160*, 3–14. [CrossRef] [PubMed]
2. Hashim, M.A.; Mukhopadhyay, S.; Sahu, J.N.; Sengupta, B. Remediation Technologies for Heavy Metal Contaminated Groundwater. *J. Environ. Manag.* **2011**, *92*, 2355–2388. [CrossRef] [PubMed]
3. Gautam, R.K.; Sharma, S.K.; Mahiya, S.; Chattopadhyaya, M.C. Contamination of Heavy Metals in Aquatic Media: Transport, Toxicity and Technologies for Remediation. In *Heavy Metals in Water: Presence, Removal and Safety*; Sharma, S.K., Ed.; The Royal Society of Chemistry: London, UK, 2015; pp. 1–24. [CrossRef]
4. Shah, G.M.; Umm-e-aiman; Imran, M.; Bakhat, H.F.; Hammad, H.M.; Ahmad, I.; Rabbani, F.; Khan, Z.U.H. Kinetics and equilibrium study of lead bio-sorption from contaminated water by compost and biogas residues. *Int. J. Environ. Sci. Technol.* **2019**, *16*, 3839–3850. [CrossRef]
5. Chowdhury, S.; Mazumder, M.A.J.; Al-Attas, O.; Husain, T. Heavy Metals in Drinking Water: Occurrences, Implications, and Future Needs in Developing Countries. *Sci. Total Environ.* **2016**, *569–570*, 476–488. [CrossRef] [PubMed]
6. Human Rights Watch. Bangladesh: 20 Million Drink Arsenic-Laced Water. Available online: https://www.hrw.org/news/2016/04/06/bangladesh-20-million-drink-arsenic-laced-water (accessed on 17 April 2017).
7. World Health Organization. Mercury and Health. Available online: http://www.who.int/mediacentre/factsheets/fs361/en/ (accessed on 17 April 2017).
8. Xu, M.; McKay, G. Removal of Heavy Metals, Lead, Cadmium, and Zinc, Using Adsorption Processes by Cost-Effective Adsorbents. In *Adsorption Processes for Water Treatment and Purification*; Bonilla-Petriciolet, A., Mendoza-Castillo, D.I., Reynel-Avila, H.E., Eds.; Springer International Publishing: Cham, Switzerland, 2017; pp. 109–138. [CrossRef]
9. Lesmana, S.O.; Febriana, N.; Soetaredjo, F.E.; Sunarso, J.; Ismadji, S. Studies on Potential Applications of Biomass for the Separation of Heavy Metals from Water and Wastewater. *Biochem. Eng. J.* **2009**, *44*, 19–41. [CrossRef]
10. Wang, J.; Chen, C. Biosorbents for Heavy Metals Removal and Their Future. *Biotechnol. Adv.* **2009**, *27*, 195–226. [CrossRef] [PubMed]
11. Park, D.; Yun, Y.-S.; Park, J.M. The Past, Present, and Future Trends of Biosorption. *Biotechnol. Bioprocess Eng.* **2010**, *15*, 86–102. [CrossRef]
12. Kurniawan, T.A.; Chan, G.Y.S.; Lo, W.H.; Babel, S. Comparisons of Low-Cost Adsorbents for Treating Wastewaters Laden with Heavy Metals. *Sci. Total Environ.* **2006**, *366*, 409–426. [CrossRef] [PubMed]
13. Londoño-Zuluaga, C.; Jameel, H.; Gonzalez, R.W.; Lucia, L. Crustacean Shell-Based Biosorption Water Remediation Platforms: Status and Perspectives. *J. Environ. Manag.* **2019**, *231*, 757–762. [CrossRef]
14. Yan, N.; Chen, X. Sustainability: Don't Waste Seafood. *Nature* **2015**, *524*, 155–157. [CrossRef]
15. Aklog, Y.F.; Egusa, M.; Kaminaka, H.; Izawa, H.; Morimoto, M.; Saimoto, H.; Ifuku, S. Protein/CaCo3/Chitin Nanofiber Complex Prepared from Crab Shells by Simple Mechanical Treatment and Its Effect on Plant Growth. *Int. J. Mol. Sci.* **2016**, *17*, 1600. [CrossRef]
16. Gagnon, B.; Berrouard, S. Effects of Several Organic Fertilizers on Growth of Greenhouse Tomato Transplants. *Can. J. Plant Sci.* **1994**, *74*, 167–168. [CrossRef]
17. Spinelli, J.; Lehman, L.; Wieg, D. Composition, Processing, and Utilization of Red Crab (Pleuroncodes Planipes) as an Aquacultural Feed Ingredient. *J. Fish. Res. Board Can.* **1974**, *31*, 1025–1029. [CrossRef]
18. Lee, M.Y.; Park, J.M.; Yang, J.W. Micro Precipitation of Lead on the Surface of Crab Shell Particles. *Process Biochem.* **1997**, *32*, 671–677. [CrossRef]
19. Percot, A.; Viton, C.; Domard, A. Optimization of Chitin Extraction from Shrimp Shells. *Biomacromolecules* **2003**, *4*, 12–18. [CrossRef] [PubMed]
20. Sagheer, F.A.; AAl-Sughayer, M.A.; Muslim, S.; Elsabee, M.Z. Extraction and Characterization of Chitin and Chitosan from Marine Sources in Arabian Gulf. *Carbohydr. Polym.* **2009**, *77*, 410–419. [CrossRef]
21. Brunauer, S.; Emmett, P.H.; Teller, E. Adsorption of Gases in Multimolecular Layers. *J. Am. Chem. Soc.* **1938**, *60*, 309–319. [CrossRef]
22. Foo, K.; Hameed, B. Insights into the Modeling of Adsorption Isotherm Systems. *Chem. Eng. J.* **2010**, *156*, 2–10. [CrossRef]
23. Abdou, E.S.; Nagy, K.S.A.; Elsabee, M.Z. Extraction and Characterization of Chitin and Chitosan from Local Sources. *Bioresour. Technol.* **2008**, *99*, 1359–1367. [CrossRef]
24. Younes, I.; Hajji, S.; Rinaudo, M.; Chaabouni, M.; Jellouli, K.; Nasri, M. Optimization of Proteins and Minerals Removal from Shrimp Shells to Produce Highly Acetylated Chitin. *Int. J. Biol. Macromol.* **2016**, *84*, 246–253. [CrossRef]
25. Karthik, R.; Meenakshi, S. Synthesis, Characterization and Cr(VI) Uptake Studies of Polypyrrole Functionalized Chitin. *Synth. Met.* **2014**, *198*, 181–187. [CrossRef]
26. Kousalya, G.N.; Gandhi, M.R.; Meenakshi, S. Preparation of Modified Chitin for the Removal of Chromium(VI). *Bioremediat. J.* **2010**, *14*, 208–218. [CrossRef]
27. Jeon, C. Adsorption Characteristics of Waste Crab Shells for Silver Ions in Industrial Wastewater. *Korean J. Chem. Eng.* **2014**, *31*, 446–451. [CrossRef]
28. Pavia, D.L.; Lampman, G.M.; Kriz, G.S.; Vyvyan, J.A. *Introduction to Spectroscopy*; Cengage Learning: Boston, MA, USA, 2014.

29. Kontoyannis, C.G.; Vagenas, N.V. Calcium Carbonate Phase Analysis Using XRD and FT-Raman Spectroscopy. *Analyst* **2000**, *125*, 251–255. [CrossRef]
30. Kawano, J.; Shimobayashi, N.; Miyake, A.; Kitamura, M. Precipitation Diagram of Calcium Carbonate Polymorphs: Its Construction and Significance. *J. Phys. Condens. Matter* **2009**, *21*, 425102. [CrossRef] [PubMed]
31. Knidri, H.; El Khalfaouy, R.; El Laajeb, A.; Addaou, A.; Lahsini, A. Eco-Friendly Extraction and Characterization of Chitin and Chitosan from the Shrimp Shell Waste via Microwave Irradiation. *Process Saf. Environ. Prot.* **2014**, *4*, 395–405. [CrossRef]
32. Julkapli, N.; Ahmad, Z.; Akil, H.M. HX-Ray Diffraction Studies of Cross Linked Chitosan With Different Cross Linking Agents For Waste Water Treatment Application. *AIP Conf. Proc.* **2010**, *1202*, 106–111. [CrossRef]
33. Teodosiu, C.; Paduraru, C.; Ibanescu, D.; Tofan, L. Biosorption of lead ions from aqueous effluents by rapeseed biomass, Irina Morosanu. *New Biotechnol.* **2017**, *39*, 110–124. [CrossRef] [PubMed]
34. Chen, P.Y.; Lin, A.Y.-M.; McKittrick, J.; Meyers, M.A. Structure and Mechanical Properties of Crab Exoskeletons. *Acta Biomater.* **2008**, *4*, 587–596. [CrossRef] [PubMed]
35. Van, H.T.; Nguyen, V.D.; Vigneswaran, S.; Nguyen, T.V.; Nguyen, L.H.; Nguyen, X.H.; Rinklebe, J.; Nguyen, T.H.; Tran, H.N. Characteristics and Mechanisms of Cadmium Adsorption onto Biogenic Aragonite Shells-Derived Biosorbent: Batch and Column Studies. *J. Environ. Manag.* **2018**, *241*, 535–548. [CrossRef]
36. Leofanti, G.; Padovan, M.; Tozzola, G.; Venturelli, B. Surface Area and Pore Texture of Catalysts. *Catal. Today* **1998**, *41*, 207–219. [CrossRef]
37. Karthik, R.; Meenakshi, S. Chemical Modification of Chitin with Polypyrrole for the Uptake of Pb(II) and Cd(II) Ions. *Int. J. Biol. Macromol.* **2015**, *78*, 157–164. [CrossRef] [PubMed]
38. Zuluaga, C.L.; Lucia, L.A.; Jameel, H.; Gonzalez, R. Marine Exoskeleton-Based Biosorption of Heavy Metals: Performance Cost Analysis. In Proceedings of the 2018 AIChE Annual Meeting, Pittsburgh, PA, USA, 28 October–2 November 2018.
39. Zuluaga, C.L.; Lucia, L.A.; Jameel, H.; Gonzalez, R. Dynamics and kinetics of marine exoskeleton-based heavy metal biosorption and desorption. In *Abstracts of Papers of the American Chemical Society*; American Chemical Society: Washington, DC, USA, 2018; Volume 255.

Disclaimer/Publisher's Note: The statements, opinions and data contained in all publications are solely those of the individual author(s) and contributor(s) and not of MDPI and/or the editor(s). MDPI and/or the editor(s) disclaim responsibility for any injury to people or property resulting from any ideas, methods, instructions or products referred to in the content.